PHYSICAL REVIEW B VOLUME 31, NUMBER 3 1 FEBRUARY 1985

Structural study of GaSb/AlSb strained-layer superlattice

C. K. Pan,* D. C. Zheng,† T. G. Finstad, and W. K. Chu
Department of Physics and Astronomy, The University of North Carolina, Chapel Hill, North Carolina 27514

V. S. Speriosu and M-A. Nicolet
California Institute of Technology, Pasadena, California 91125

J. H. Barrett
Solid State Division, Oak Ridge National Laboratory, Oak Ridge, Tennessee 37830
(Received 11 June 1984)

Owing to the lattice mismatch between GaSb and AlSb, a superlattice consisting of alternating layers of these materials will be strained. We have carried out ion-channeling measurements by backscattering of 1.76-MeV He ions, and present an experimental procedure and a data-analysis technique to measure the difference in strain between the two individual layers of the superlattice. The data analysis is based on computer simulations of channeling, the accuracy of which is supported by the many fine details of the experiments reproduced in the simulations. X-ray rocking-curve analysis yielded detailed profiles of strains in directions perpendicular and parallel to the surface. The x-ray value for the strain present at an unirradiated spot on the crystal is in excellent agreement with the value calculated by elasticity theory. In the bombarded region, the values of strain are less than the value calculated by elasticity theory. It appears that bombardment by the He ions reduced the strain by 50% and created lateral inhomogeneities in the crystal structure.

I. INTRODUCTION

Superlattices fabricated by the epitaxial growth of alternating layers of two different semiconductors constitute a group of materials with unique electrical and optical properties. The introduction of lattice-mismatched superlattices[1] has broadened this group of materials. Under certain circumstances, the lattice mismatch in these systems will be accommodated by an approximately uniform strain.[1–3] This makes it possible to use a larger variety of semiconductor materials in the alternating layers. Moreover, the strain in each individual layer can be used to modify the intrinsic physical properties, and the structures are also of interest for zone-folding experiments. It is well known that there exists some maximum thickness of a lattice-mismatched epitaxial overlayer above which dislocations develop and the strain is less than for thinner layers. In equilibrium this can be predicted; however, it is not yet clear where these limits will be for the different specific growth conditions used to fabricate various superlattices. Furthermore, it is not clear how stable these structures will be. For these reasons, strain measurements on superlattices are an important task in the characterization of these materials.

Ion-beam channeling and x-ray diffraction have proven to be valuable tools for characterizing strained-layer superlattices. X-ray diffraction has provided detailed depth profiles of perpendicular strain in AlAs/GaAs superlattices.[4,5] The first investigation of strained superlattices with the backscattering channeling method was carried out on a GaSb/InAs superlattice structure.[6,7] Recently, various different methods for the characterization and measurement of the strain in superlattices have been developed.[8–11]

We have previously reported on the channeling measurement of strain in a GaSb/AlSb superlattice.[8] The measurement was based upon the fact that, for a superlattice grown along the [100] direction, the "angle for best channeling" along the [110] direction will be different for the individual layers in the superlattice. The difference between the angle for best channeling of the first and second layers was measured to be $0.17°\pm0.03°$. If the lattice mismatch is completely accommodated by strain in the layers, one can calculate the magnitude of the angle between the [110] axes of two layers from elastic constants and lattice parameters of the individual layers. We named that a "kink angle."

In this paper we will elaborate on the channeling measurements briefly reported earlier[8] and also include x-ray rocking-curve analysis and computer simulations of the same GaSb/AlSb superlattice sample. A comparison between the results and an evaluation of the methods used will be given.

II. EXPERIMENTAL PROCEDURES

The layered structure of the sample used in this investigation is given in Fig. 1. The sample was a GaSb/AlSb (30 nm/30 nm) periodic structure with a total of 10 periods. The films were grown by molecular-beam epitaxy. A 2-μm-thick GaSb buffer layer was first grown on a GaSb[100] substrate to smooth the surface. Details of the growth procedure have been given elsewhere.[12]

Figure 2 shows a schematic model of a strained-layer superlattice. The GaSb layer is unstrained due to its con-

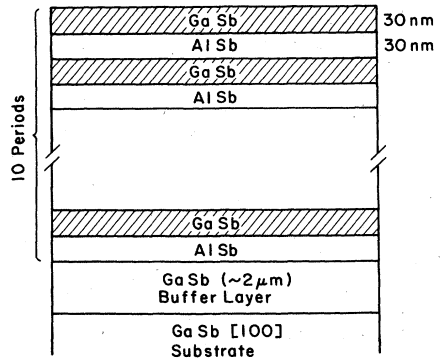

FIG. 1. Configuration of a strained-layer superlattice GaSb/AlSb.

formity with the substrate. When layers with different lattice constants are grown on top of each other and the interface atoms are in registration, the lattice constant perpendicular to the growth direction will be different for the two layers. A detailed discussion of the lattice constants and strains in the layers will be given in Sec. III. When the growth is along the [100] direction, the strain will cause the [110] crystallographic direction to be different for the two layers. Consequently, a "kink angle" is developed.

Ion backscattering and channeling is well described by several authors.[13,14] In this investigation, backscattering of 1.76-MeV $^4He^+$ ions with a scattering angle of 162° was used. Figure 3 shows schematically the situation when the sample is aligned so that the beam is along the [110] direction. As shown in the figure, the [110] axis is kinked at each interface of the superlattice. The channeling measurements in this work consist of collecting backscattering spectra for several incident directions separated by small angles, all lying in a plane containing the [110] axis.

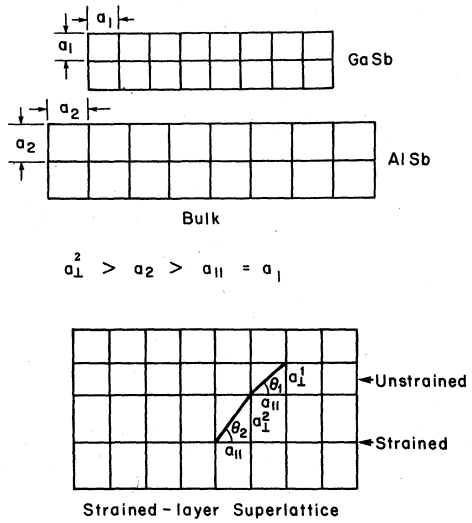

FIG. 2. Schematic diagram of the layers of a GaSb/AlSb sample. The lattice distortion of AlSb due to mismatch to the substrate is shown.

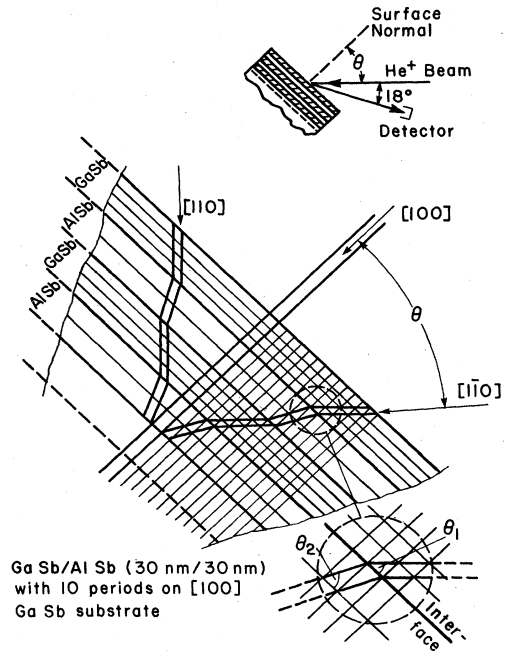

FIG. 3. Difference in channeling directions between [110] directions in two adjacent layers due to the strain.

For aligning the crystal with one of the ⟨110⟩ axes we use a two-axis goniometer with a rotational axis designated ϕ and a tilt angle designated θ. The axis of rotation is perpendicular to the surface and the tilt axis is in the surface plane and perpendicular to the beam direction. Figure 4 shows part of a polar diagram of crystallographic axes and planes in a coordinate system tied to the experimentally recorded tilt and rotation angles.

The major crystallographic planes shown in Fig. 4 are first found from monitoring "dips" in the backscattering intensity when the sample is rotated and the surface normal is tilted several degrees away from the beam direction. The minima found in this way are then plotted in a polar diagram where the coordinate system is defined by

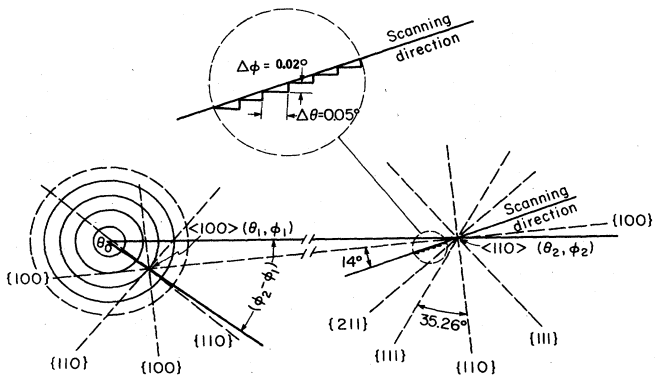

FIG. 4. Polar-coordinate diagram to illustrate the exact directions in the channeling experiments. The scanning direction 14° away from a {100} plane is also shown.

the tilt angle θ and the rotation angle ϕ. A $\langle 100 \rangle$ axis is then found by setting the goniometer to the intersection of lines through these points, followed by a fine tuning. Then a $\langle 110 \rangle$ axis is found by sliding along a $\{100\}$ plane until the minimum is found close to a $\langle 110 \rangle$ direction. This corresponds to the minimum scattering intensity averaged over several superlattice periods. The actual angular scan is then performed by varying both θ and ϕ for each step in the scan so that the angular scan plane does not coincide with any major crystallographic planes. The chosen scan direction in our experiments made an angle of 14° to a $\{100\}$ plane. The exact angle in the crystal between the $\langle 100 \rangle$ and $\langle 110 \rangle$ directions cannot be precisely determined in our measurements since small inaccuracies in the experimental setup could influence this. However, the precision in measuring small differences between angles is very good ($\pm 0.02°$). Details on the channeling-data—reduction procedures will be given in Sec. IV.

The same samples used in the channeling measurements were also characterized by x-ray rocking-curve analysis. Details about experimental procedure to characterize the depth distribution of strain in strained-layer superlattices have previously been described.[4,5,15–17] In this investigation, a double-crystal diffractometer with Fe $K\alpha_1$ radiation was used. A [100] GaAs crystal was used as the first crystal, with (400) reflections for both sample and first crystal. The experimental data are analyzed by comparison with computer-calculated reflection intensities.[15] The computer program assumes a certain strain distribution with depth, and scattered x-ray intensities are modeled by kinematical theory, which is a good approximation under the present circumstances. A detailed discussion of x-ray analysis of superlattices and additional information on measurements of the present samples is given elsewhere.[18]

III. STRAIN CALCULATIONS

In this section we present the values for the expected lattice constant in the superlattice structure under study, and also the expected values for the angle between the [110] directions of each of the layers in the superlattice based on the elasticity theory of layered structures.

GaSb and AlSb, which contribute the individual layers in the superlattice, both have the zinc-blende crystal structure, and their lattice constants are only slightly different from each other. In Fig. 2, a_1 and a_2 are the bulk lattice constants for GaSb and AlSb, respectively. a_2 is slightly larger than a_1. The lattice mismatch f, defined by

$$f=\frac{2(a_2-a_1)}{a_2+a_1}, \tag{1}$$

is 0.65%.

When a thin layer is grown on the substrate, atoms will register at the atoms of the substrate. The lattice constant $a_{\parallel}$ in the growth plane (Fig. 2) will then conform to that of the substrate. As the substrate is much thicker than the layers in the superlattice, the changes in the lattice constant of the substrate will be insignificant. Thus, the AlSb layers in the superlattice will register with a parallel lattice constant close to that of the substrate (i.e., $a_{\parallel} \approx a_1$). The lattice constant perpendicular to the plane $a_{\perp}$ can be calculated from the Poisson effect,

$$\begin{aligned} a_{\perp}^{(1)}-a_1&=-2\left[\frac{C_{12}}{C_{11}}\right]_{\text{GaSb}}(a_{\parallel}-a_1), \\ a_{\perp}^{(2)}-a_2&=-2\left[\frac{C_{12}}{C_{11}}\right]_{\text{AlSb}}(a_{\parallel}-a_2), \end{aligned} \tag{2}$$

where, $a_{\perp}^{(1)}$ and $a_{\perp}^{(2)}$ are the lattice constants perpendicular to the plane for GaSb and AlSb, respectively. C_{11} and C_{12} are the elastic stiffnesses corresponding to stress along the growth direction and a direction in the growth plane, respectively. In our case, the GaSb layer can be practically unstrained since $a_{\parallel}$ is very close to a_1.

The directions of [110] axes of the strained layers are changed, while no change occurs in the unstrained layers with respect to the [110] axis of the substrate. The angle $\Delta\theta$ between the [110] axis of the two different layers can be calculated from

$$\Delta\theta=\theta_2-\theta_1=\arctan\left[\frac{a_{\perp}^{(2)}}{a_{\parallel}}\right]-\arctan\left[\frac{a_{\perp}^{(1)}}{a_{\parallel}}\right]. \tag{3}$$

$\Delta\theta$ is the "kink angle," which is a way to express the strain of the system, and θ_2 and θ_1 are defined in Fig. 2.

A tabulation of calculated values of the "kink angles" for the superlattice under study is shown in Table I for two different values of the lattice constant of GaSb cited in the literature. We expect the lattice parameter of Ref. 19, which is in agreement with the published value of the National Bureau of Standards (NBS), to be a more accurate one. A similar calculation, assuming that both layers of the superlattice are strained, as would have been the case if the growth had started with an infinitesimally thin substrate or with a buffer layer decoupling the superlattice layer from the substrate completely, does not make any

TABLE I. Lattice constant and "kink-angle" calculation.

a_1(GaSb) (Å)	a_2(AlSb) (Å)	$a_{\parallel}$(GaSb) (Å)	$a_{\perp}^{(1)}$(GaSb) (Å)	$a_{\perp}^{(2)}$(AlSb) (Å)	$\Delta\theta$ ("kink angle") (deg)
6.095[a,b]	6.135[a]	6.095	6.095	6.175	0.374
6.118[c]	6.135	6.118	6.118	6.152	0.159

[a]Reference 19.
[b]Lattice parameter of Ref. 19 is believed to be more accurate.
[c]Reference 20.

significant difference in the value of the calculated "kink" angle $\Delta\theta$. Experimental measurement of the "kink angle" is given in the next section.

IV. CHANNELING MEASUREMENTS

Figure 5 shows some typical experimental backscattering spectra from the GaSb/AlSb superlattice. The oscillations seen in the scattering yield in the spectra are due to the variation in composition with depth. The spectrum labeled "[100] aligned" was obtained with the analysis beam incident along the [100] direction of the superlattice. The one labeled "[110] aligned" was obtained by the analysis beam incident along the average [110] direction of the superlattice layers. They indicate that the dechanneling is higher along the [110] direction than along the [100] direction, as is normally observed in strained-layer superlattices.[6–10] The spectrum labeled "random" was obtained with the incident-beam direction making an angle of 3° with the [110] axis and 10° with the $(1\bar{1}0)$ plane. For the measurements of the "kink angle," we collected a large number of individual spectra, all with the beam direction lying in a plane that makes an angle of 14° with a {100} plane, as indicated in Fig. 4. The angular difference between the analysis direction for consecutive spectra was 0.05° or 0.1°. Figure 5 shows three out of a total of 52 such spectra. Since the energy scale in Fig. 5 can be converted to a depth scale, the above-mentioned data allow us to plot the yield at different depths as function of tilt angle from the [110] axis of the first layer. In Fig. 5, the energy intervals corresponding to the individual GaSb (layers 1, 3, and 5) and AlSb (layers 2, 4, and 6) have been indicated for the Sb part of the spectrum (1.4—1.6 MeV) and for the superimposed contribution from Ga and Sb (below 1.4 MeV). The energy positions for each individual layer have been assumed to be identical for a random direction and an aligned direction, neglecting differences in stopping cross section and energy straggling for the random and aligned cases. For the purpose of converting the energy scale to a depth scale, this is a reasonable approximation.

Figure 6 shows angular yield curves extracted from experimental measurements, such as Fig. 5, at four different depths. The yields have been normalized to the random yield. From each of these curves, we find an angular position termed the direction or angle for "best channeling" for a given depth. It is defined as the midposition between the intercept of half-heights of the left- and right-hand portions of the angular yield curve, respectively. This parameter serves to quantify the observed effect.[8] It is interesting to note that the direction for "best channeling" shifts back and forth from layer to layer in the superlattice. We attribute the observed periodic changes in the angular yield curves to the periodic changes of the [110] direction in the superlattice structure.

Figure 7 shows the angular position of the best-channeling direction as a function of depth. The depths corresponding to the individual layers are also indicated in the figure. The error bars are typical for all the data points. Data points of layers deeper than the fourth layer are somewhat doubtful since they have been extracted from portions of the spectrum where the Ga signal from one depth overlaps the Sb signal from other depth. One

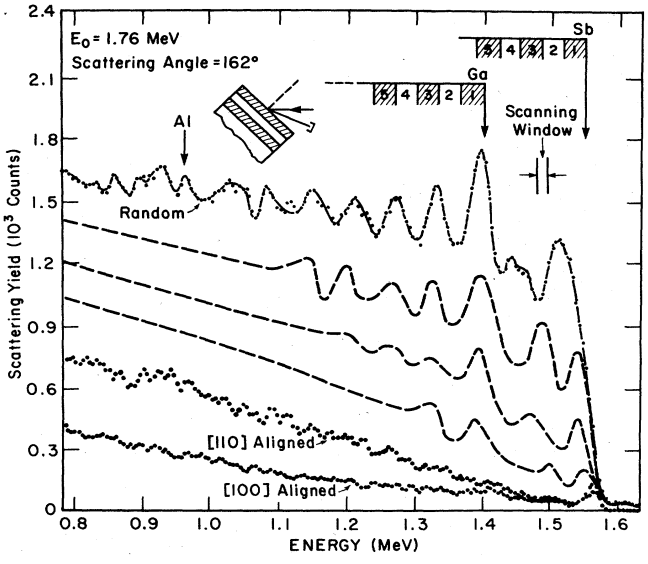

FIG. 5. Energy spectra of 1.76-MeV He^+ ions backscattered from [100] GaSb/AlSb superlattices. Depth scales based on both Sb and Ga signals are marked in units of the number of layers (30 nm per layer), [100]- and [110]-aligned spectra, and a random spectrum taken at an angle of 3° with respect to the [110] direction, and three more spectra between the [110] and random spectra are given.

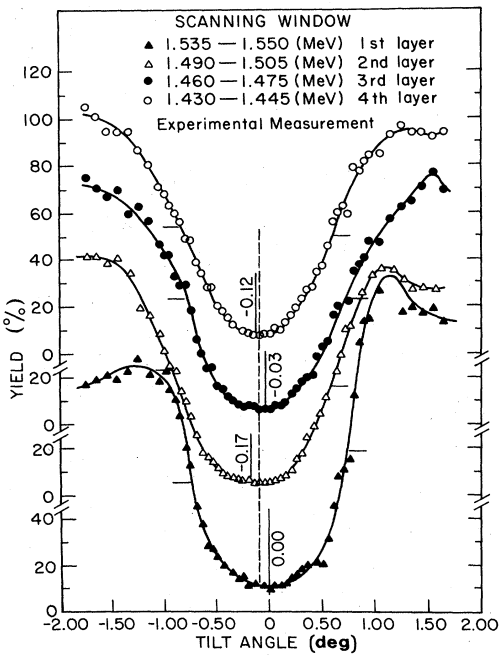

FIG. 6. Angular scan done by setting an energy window from the first to fourth layer from 52 spectra run at 52 different angles. The center position of the angular scan changes from layer to layer, indicating that the [110] direction varies. The vertical dashed line is the limiting center position for layers much deeper in the specimen.

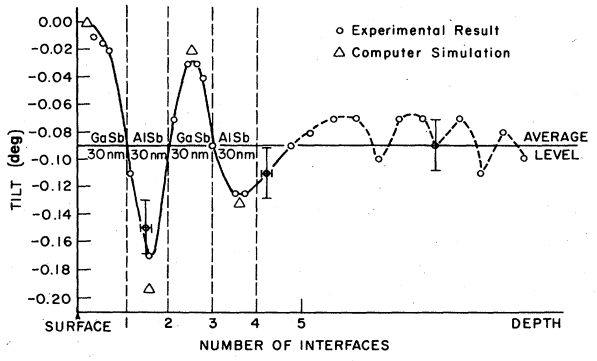

FIG. 7. Oscillation of the angular position of minimum yield plotted as a function of depth. Both experimental results and computer simulation are shown.

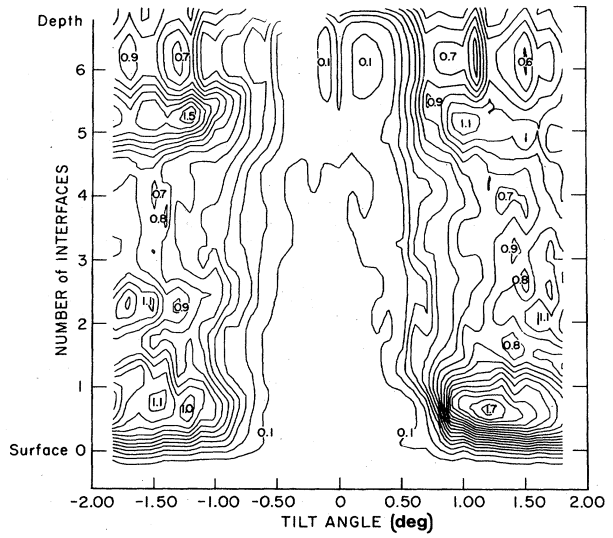

FIG. 8. Monte Carlo simulation backscattering probability contours for 1.76-MeV He ions in GaSb/AlSb. The "kink angle" assumed was 0.37°. The level of local maxima and minima are shown, and the interval between contours is 0.1.

can see from Fig. 7 that the damping of the oscillations is quite clear. This damping occurs because the ions become increasingly insensitive after passage through many layers to the direction of the layer they are in, and the direction for best channeling tends towards a steady value determined by the cumulative history through the layers nearer the surface. This steady value will have a complex dependence on the relationship of the wavelength of the ions within the layers to the path length through the different layers. The only simple situation which is known to occur[2] is for layers that are very thin compared to the wavelength, in which case the direction for best channeling is an average of the directions in the two types of layers. The observed differences between the best-channeling direction for the first two layers is 0.17° ±0.03°, which should be a lower limit for the "kink angle." These findings will be compared with the computer-simulation and the x-ray rocking-curve measurements.

V. COMPUTER SIMULATIONS

Monte Carlo simulations of ion channeling in the crystal can be used to infer more precise information from measurements. A description of such computer simulation has been given previously[2,21] and applied to the analysis of experiments[6,7] on InAs/GaSb superlattices. Only one modification has been added to that program for the present purposes; this modification is for the purpose of keeping separate records of ion encounters with the group-III and -V atoms in each layer. This feature turns out to be important in reproducing the correct shapes for the shoulders in angular scans such as that observed in Fig. 6.

Figure 8 shows the contour diagram of a Monte Carlo simulation run on GaSb/AlSb. The contour levels over the depth—incident-angle plane are of scattering probabilities. The "kink angle" for Fig. 8 was chosen to be 0.37° for the simulation. It is quite evident that the contours of Fig. 8 are asymmetric with respect to the angle of incidence. Figure 9 shows the contour diagram of a simulation assuming zero "kink angle." It is seen therein that the major asymmetry due to "kink angle" is not apparent, although minor asymmetry due to ions incident close to group III as opposed to V is present. The simulation scanning profiles shown in Fig. 10 were extracted from the data of the contour diagram at the different depths given in Fig. 8. One can see that the angle for best channeling as previously defined oscillates with depth, in good agreement with our experiments (see Fig. 7), and tends to a steady value at greater depths, as expected. We have done other simulations with other "kink angles," but with all other parameters unchanged. Figure 11 shows the angle difference $\Delta\psi$ between the "direction for best channel-

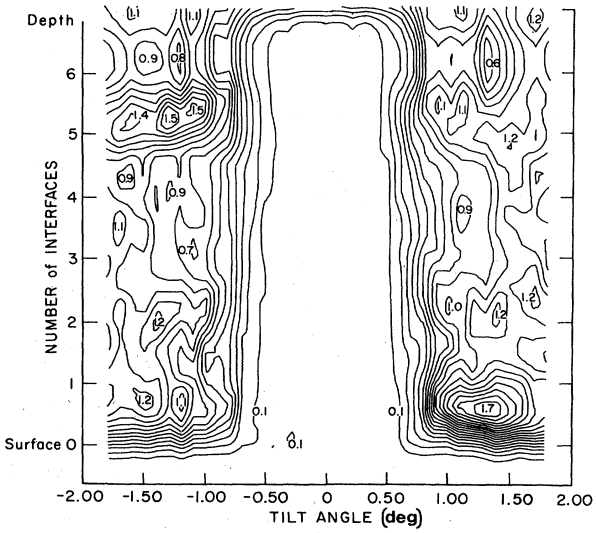

FIG. 9. Monte Carlo simulation backscattering probability contours for 1.76-MeV He ions in GaSb/AlSb. The "kink angle" assumed was zero. The level of local maxima and minima are shown, and the interval between contours is 0.1.

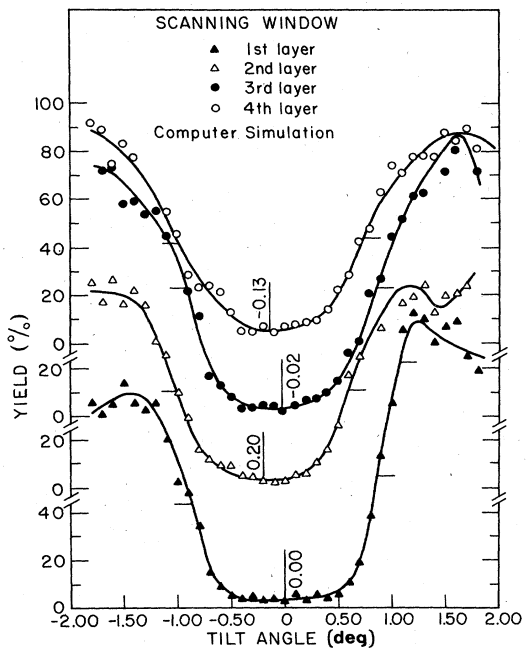

FIG. 10. Angular scan profiles abstracted from the computer simulation of Fig. 8 for the first four layers of GaSb/AlSb under the same depth conditions as those in the experiments (Fig. 6).

ing" of the first and second superlattice layers as a function of assumed "kink angles" $\Delta\theta$. It is noted that the angle difference between first and second layer is always somewhat smaller than the assumed "kink angle." One can use Fig. 11 to extract the "kink angle" from the channeling measurements. It should be noted that the tilt angles in Figs. 6 and 7 are different from those in Figs. 8—10. In Figs. 6 and 7, "tilt angle only" denotes the change in θ, while "tilt angle" denotes the real change from the combination of θ and ϕ in Figs. 8—10. For comparison between the values of the tilt angles, the scale should be enlarged by 3.8% in Figs. 6 and 7. The percentage was obtained from a simple geometric consideration. The formula we derived is as follows:

$$\cos(\Delta\Psi)=\cos(\Delta\theta)\cos(\Delta\phi)+\cos(\theta_2)\cos(\theta_1)[1-\cos(\Delta\phi)]\ ,$$

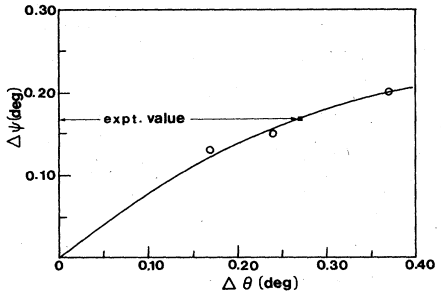

FIG. 11. Angle difference ($\Delta\psi$) between "directions for best channeling" of the first and second layers, plotted as a function of assumed "kink angle" $\Delta\theta$.

where $\Delta\psi$ is tilt angle in Figs. 8—10. $\Delta\theta$ is tilt angle in Figs. 6 and 7. $\theta_1\sim45°$ is the angle between the beam direction and the ϕ rotatory axis of the goniometer during the experimental angular scan. $\theta_2\sim45°$ is an angle between the ⟨100⟩ axis and the average ⟨110⟩ axis. The experimentally measured value for $\Delta\psi$ was 0.176°. From Fig. 11 this corresponds to a "kink angle" of 0.28°±0.04°. The shoulders of the simulated scan profiles in Fig. 10 reproduce the shoulders of the experimental ones in Fig. 6 in great detail. This close agreement gives strong support to the use of the simulations to make quantitative inferences from the measurements. Almost the only way in which the two sets of scans differ is that the simulated profiles are somewhat broader and flatter-bottomed than the experimental ones, a difference that is typical of such comparisons.[22] In the present comparison there may be specific contributions to this difference from not using the correct thermal-vibration amplitudes or not including, in the simulations, the effects of surface roughness, surface oxide, beam divergence, or defects in the superlattice.

VI. X-RAY ROCKING-CURVE MEASUREMENTS

The x-ray measurements were performed on the same sample as the channeling measurements. A large difference in structure was found between data taken on the Rutherford-backscattering (RBS) spot, i.e., the spot bombarded by the He beam during the channeling measurements, and data taken a few millimeters away. Figure 12 shows the experimental (dashed curve) and calculated (solid curve) Fe $K\alpha_1$ (400) rocking curves for an unirradiated spot away from where the channeling measurements were taken. Since there is no phase detection, a direct inversion of an experimental rocking curve into a strain profile is not possible. Instead, a strain-versus-depth profile is first assumed, and a computer program then calculates the expected x-ray-intensity variations. When a good fit is obtained, it is assumed that the correct strain profile has been found. It should be mentioned that the calculations are very sensitive to small differences in assumed

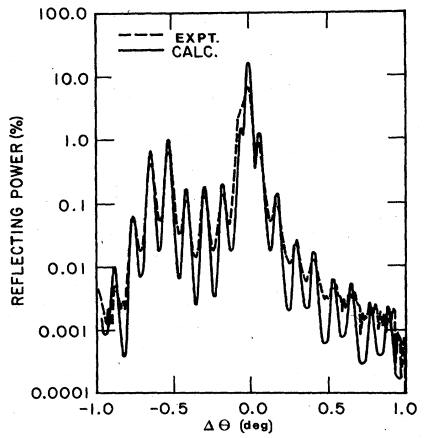

FIG. 12. Experimental (dashed curve) and calculated (solid curve) Fe $K\alpha_1$ (400) x-ray rocking curves of GaSb/AlSb superlattice on the unirradiated spot.

strain profiles ($\sim 1\%$). The strain is defined here with respect to the lattice constant a_1 of the substrate: For parallel strains,

$$\epsilon_{||}^{(1)}=\frac{a_{||}^{(1)}-a_1}{a_1},\quad \epsilon_{||}^{(2)}=\frac{a_{||}^{(2)}-a_1}{a_1},$$

and for perpendicular strains, (4)

$$\epsilon_{\perp}^{(1)}=\frac{a_{\perp}^{(1)}-a_1}{a_1},\quad \epsilon_{\perp}^{(2)}=\frac{a_{\perp}^{(2)}-a_1}{a_1},$$

where the superscripts (1) and (2) denote GaSb and AlSb separately. The best fit was constructed from a profile using 10 periods of GaSb(30 nm)/AlSb(30 nm) with a perpendicular strain of 1.25% and -0.03% in the AlSb and GaSb layers, respectively. Symmetric reflections, such as the (400), are sensitive only to perpendicular strain. Asymmetric reflections are sensitive to $\epsilon_{\perp}$ and $\epsilon_{||}$, and combination with symmetric reflections produces values for both. Using Fe $K\alpha_1$ (422) reflections, a uniform $\epsilon_{||}=(+0.03\pm 0.02)\%$ was measured throughout the superlattice.[18]

Since the cross section of the x-ray beam can be confined by slits to less than 1 mm^2, we can analyze different areas of the surface. In particular, we were able to perform the analysis of the same spot where the channeling measurement had been carried out, since this (RBS) spot is clearly visible, probably due to cracking of diffusion-pump oil by the He beam during the channeling analysis. Because of the amorphous structure and limited thickness of this layer, it should not have any effect on the strain in the underlying superlattice. The experimental rocking curve on the RBS spot is shown in Fig. 13. The structure of the experimental rocking curve indicates that the strain in the AlSb layer is about half of what it is for the unirradiated spot. The reduction in the intensities of peaks located away from zero angle is due to broadening caused by lateral nonuniformities in the sample. The x-ray rocking-curve data and channeling data are summarized in Table II. The value of strain in the GaSb layers is so small that it can be considered to be zero in the theoretical calculation like the one we did previously.

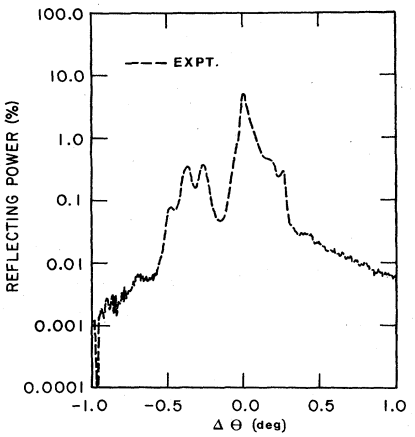

FIG. 13. Experimental x-ray Fe $K\alpha_1$ rocking curve of GaSb/AlSb superlattice on the RBS-investigated spot.

TABLE II. Experimental results.

	X ray[a]	X ray[b]	RBS
$\epsilon_{\perp}^{(1)}$ (%)	-0.03	~ 0	(0)
$\epsilon_{\perp}^{(2)}$ (%)	1.25	~ 0.6	0.98 ± 0.14
$\epsilon_{||}^{(1)}$ (%)	0.03	~ 0	(0)
$\epsilon_{||}^{(2)}$ (%)	0.03	~ 0	(0)
$\Delta\theta$ ("kink angle") (deg)	0.365 ± 0.004	~ 0.17	0.28 ± 0.04

[a]On unirradiated spot.
[b]On RBS spot.

VII. DISCUSSION

We have studied GaSb/AlSb superlattice structures by a combination of channeling scans and computer simulations, and by x-ray rocking-curve measurements.

The value of the "kink angle" detected by x-ray on an unirradiated spot is in good agreement with an elasticity calculation. However, on the spot used for channeling measurements, the value of the "kink angle" detected by x-ray is different from that obtained by channeling scans combined with computer simulation. It is reasonable to assume that the He bombardment has caused structural changes in the superlattice. We should mention that in the present case much of the bombardment was done on the sample during test runs and during the alignment procedures of crystal before the channeling scans. In addition, further ion-scattering experiments were made on the same sample after the channeling scans and before the x-ray measurements. Our results reveal that the strain in the superlattice is slowly released during mega-electron-volt ion bombardment. It would be highly desirable to ascertain the critical dose below which channeling can measure the actual strain in a certain superlattice without perturbing it. The damage-production mechanism is not clear. The initial mechanism could be direct knock-on (nuclear stopping) to create Frenkel pairs, or the effect of ionization in bond breaking. The generation of vacancies could facilitate intermixing of the individual layers, although no evidence for this has been observed by us. Our observation on the change of strain may help to answer questions about how stable these strained-layer superlattices are. There have been several reports on degradation of strained superlattice layers. Ludowise *et al.*[23] reported upon continuous (CS) 300-K laser operation of a $GaAs/In_xGa_{1-x}As$ ($x\sim 0.2$) superlayer with a strain of 0.7% and of a $GaAs_{1-x}P_x/GaAs$ ($x\sim 0.25$) layer with a strain of 0.45%. The superlattice with the lowest stress had the lowest failure rate.

VIII. CONCLUSIONS

From our channeling and x-ray-diffraction measurements on strained-layer superlattices of AlSb/GaSb, we conclude the following.

(1) X-ray rocking-curve analysis is a very powerful method for characterizing the strain in superlattices as a function of depth, since it determines the geometry of the distortion (parallel, perpendicular, negative, or positive

strain). The strain determined by this method is in excellent agreement with that calculated from the elastic constants and lattice misfit of the layer materials.

(2) Backscattering and channeling measurements, combined with computer simulation, also allow a determination of the strain by providing a value of the associated "kink angle." The strain determined in this way is in reasonable agreement with the x-ray and elastic-misfit values.

(3) He-ion-beam bombardment at extended doses relieves a large portion of the strain of the AlSb/GaSb strained superlattice. This limits the beam dose that can be used in ion-backscattering measurements without perturbing the specimen. On the other hand, this ion-beam perturbation might be utilized to modulate strain in superlattices in a controllable manner. This has potential processing applications in integrated optics involving superlattice layered structures.

ACKNOWLEDGMENTS

The authors would like to thank S. T. Picraux for valuable discussions regarding channeling and elasticity, as well as E. Frey and D. Y. Han for assistance of the data reduction. The superlattice sample used in this work is identical to that used in Ref. 8. We acknowledge C.-A. Chang of the IBM Corporation for making such a sample available to us. Part of the work was supported by the Microelectronics Center of North Carolina. At the California Institute of Technology, two of us (V.S.S. and M-A.N.) would like to acknowledge the support of the Defense Advanced Research Projects Agency under Contract No. MDA-903-82-C-0348 (S. Roosild). Research performed at Oak Ridge National Laboratory was sponsored by the Division of Materials Sciences, U.S. Department of Energy, under Contract No. DE-AC05-840R21400 with Martin Marietta Energy Systems, Inc.

---

*Permanent address: Jiangxi Engineering College, Jiangxi, China.

†Permanent address: Jiangxi Education College, Jiangxi, China.

[1]G. C. Osbourn, J. Appl. Phys. **53**, 1586 (1982).

[2]J. H. Barrett, Phys. Rev. B **28**, 2328 (1983).

[3]J. W. Mathews and A. E. Blakeslee, J. Vac. Sci. Technol. **14**, 989 (1977).

[4]A. Segmüller, P. Krishna, and L. Esaki, J. Appl. Crystallogr. **10**, 1 (1977).

[5]R. M. Fleming, D. B. Mewhan, A. C. Gossard, W. Wiegmann, and R. A. Logan, J. Appl. Phys. **51**, 357 (1980).

[6]F. W. Saris, W. K. Chu, C.-A. Chang, R. Ludeke, and L. Esaki, Appl. Phys. Lett. **37**, 931 (1980).

[7]W. K. Chu, F. W. Saris, C.-A. Chang, R. Ludeke, and L. Esaki, Phys. Rev. B **26**, 1999 (1982).

[8]W. K. Chu, C. K. Pan, and C.-A. Chang, Phys. Rev. B **28**, 4033 (1983).

[9]S. T. Picraux, L. R. Dawson, G. C. Osbourn, and W. K. Chu, Appl. Phys. Lett. **43**, 930 (1983).

[10]S. T. Picraux, L. R. Dawson, G. C. Osbourn, R. M. Biefeld, and W. K. Chu, Appl. Phys. Lett. **43**, 1020 (1983).

[11]W. K. Chu, J. A. Ellison, S. T. Picraux, R. M. Biefeld, and G. C. Osbourn, Phys. Rev. Lett. **52**, 125 (1984).

[12]C. A. Chang, H. Takaoka, L. L. Chang, and L. Esaki, Appl. Phys. Lett. **40**, 983 (1982).

[13]W. K. Chu, J. W. Mayer, and M-A. Nicolet, *Backscattering Spectrometry* (Academic, New York, 1978).

[14]L. C. Feldman, J. W. Mayer, and S. T. Picraux, *Materials Analysis by Ion Channeling* (Academic, New York, 1982).

[15]V. S. Speriosu, J. Appl. Phys. **52**, 6094 (1981).

[16]V. S. Speriosu and C. H. Wilts, J. Appl. Phys. **54**, 3325 (1983).

[17]V. S. Speriosu, M-A. Nicolet, S. T. Picraux, and R. M. Biefeld (unpublished).

[18]V. S. Speriosu and T. Vreeland, Jr., J. Appl. Phys. (to be published).

[19]Marvin K. Farr, J. G. Traylor, and S. K. Sinha, Phys. Rev. B **11**, 1587 (1975).

[20]D. S. Gemmel, Rev. Mod. Phys. **46**, 129 (1974).

[21]J. H. Barrett, Phys. Rev. B **3**, 1527 (1971).

[22]See, for instance, Fig. 3 in J. H. Barrett, Nucl. Instrum. Methods **149**, 341 (1978).

[23]M. J. Ludowise, W. T. Dietze, C. R. Lewis, M. D. Camres, N. Holonyak, Jr., B. K. Fuller, and M. A. Nixon, Appl. Phys. Lett. **42**, 487 (1983).